

# 28 GHz Propagation Measurement Using FMCW Radar in a Reverberation Chamber (Invited paper)

MyungHun Jeong<sup>1</sup>, KiBeom Kim<sup>1</sup>, DaeHwan Jung<sup>1</sup>, and SeongOok Park<sup>1</sup>

<sup>1</sup>Department of Electrical Engineering, KAIST,  
335 Gwahak-ro, Yuseong-gu, Daejeon 305-701, Republic of Korea

**Abstract** – The radio propagation characteristics of 28 GHz were investigated by using a FMCW (Frequency Modulated Continuous Wave) radar system in a reverberation chamber for the small-fading of Rayleigh and Rician conditions.

**Index Terms** — FMCW, reverberation chamber, Rayleigh fading, Rician fading

## I. INTRODUCTION

The shipments of smart connected devices (PC, smart phone, and tablet) have rapidly increased in global. In order to tolerate the heavy data traffic, the millimeter wave frequency spectrum offers innovative bandwidths for future broadband cellular networks [1][2]. Especially, the mm-wave band of 28GHz is suitable for outdoor mobile communication as the atmospheric absorption does not significantly contribute to additional path loss [1]. It is known to be quite a challenge to figure out the radio propagation of 28 GHz.

A FMCW radar is commonly used to sound wireless channel due to such advantages as system stability and uniform measurement system [3][4]. In this paper, we show the propagation characteristics of 28 GHz using FMCW radar in a reverberation chamber in that Rayleigh and Rician fading can be emulated.

## II. FMCW RADAR FOR CHANNEL SOUNDER

The FMCW radar emits a radio frequency signal that is usually swept linearly in the time domain. A frequency difference between the received signal and transmitted signal increases the delay, and that means propagation distance. It is obtained by mixing with the received and transmitted signals, hence it can be detected as an IF signal ( $S_{IF}$ ).

In the LFM (Linear Frequency Modulation) technique, the IF signal of the FMCW radar is demonstrated in terms of time and frequency domain signals. As the change of the sweep time corresponds to the change of the frequency in the LFM, the time domain signal is simultaneously represented in the frequency domain signal without Fourier transform [4]. The scattering parameter,  $S_{21}$ , in the radio channel is proportional to the conjugate of the IF signal,  $S_{IF}$ . The relationship between  $S_{21}$  and  $S_{IF}$  can be expressed as follows,

$$S_{21}(F_i) = k \cdot [S_{IF}(F_i)]^*, \quad (t = \frac{i}{N-1} T_m) \quad (1)$$

where  $k$  is an arbitrary constant,  $*$  denotes the conjugate operation,  $N$  is the number of sweep frequencies in the sweep period, and  $T_m$  is the modulation time.

The channel impulse response is extracted from the measured channel frequency response by performing an IDFT (Inverse Discrete Fourier Transform) of  $S_{21}$  [5]. The normalized impulse response of the system is defined by the DFT (Discrete Fourier Transform) of  $S_{IF}$ ; because the IDFT of the  $S_{21}$  corresponds to the conjugated DFT of  $S_{IF}$ .

$$\begin{aligned} h_{norm}(\tau, m) &= \frac{IDFT[S_{21}(F_i, m)]}{\max(\text{abs}\{IDFT[S_{21}(F_i, m)]\})} \\ &= \frac{\{DFT[S_{IF}(F_i, m)]\}^*}{\max(\text{abs}\{DFT[S_{IF}(F_i, m)]\})^*} \end{aligned} \quad (2)$$

With this result, the normalized PDP (Power Delay Profile) can be defined by the impulse response as follows [6],

$$PDP(\tau) = \frac{\langle |h_{norm}(\tau, m)|^2 \rangle}{\max[\langle |h_{norm}(\tau, m)|^2 \rangle]} \quad (3)$$

where  $\langle \rangle$  is the average operator.

In this paper, the FMCW radar is based on PLLs (Phase Locked Loops) and a DDS (Direct Digital Synthesizer) for LFM. All PLLs are synchronized using the stable 10-MHz clock source, and the DDS (AD9854) sweeps the frequency linearly. The FMCW radar operates at 28108.5MHz; the sweep bandwidth and time are 200MHz and 50 $\mu$ s.

## III. EXPERIMENT AND RESULTS

The measurement campaigns including the positions of absorbers, mode stirrer, TX (Transmitting) and RX (Receiving) system, are shown in Fig. 1. The mode stirrer rotates in the CCW direction with 400 steps; step angle of 0.9 degree, and the number of sampled data is 1000 for the each stirred position using the oscilloscope (Agilent DSO7104A).

The TX and RX antennas for the FMCW radar have vertical polarization and 90 degree beamwidth. For the Rayleigh fading channel, the TX antenna is faced to the mode stirrer, and this electromagnetic field scatters randomly in the reverberation chamber. The RX antenna is orthogonally located to the TX antenna in order to avoid the direct radio path.

On the contrary, the TX and RX antenna are placed at the angles  $\phi_{TX}=30^\circ$  and  $\phi_{RX}=60^\circ$  for the Rician environment. When the TX and RX antenna were placed face to face in the same plane for the LOS condition, the scatters were very weak and the direct coupling component was significantly strong.

In order to analyze the 28GHz propagation in the various radio environments, the absorber is placed at the specific position in several scenarios.

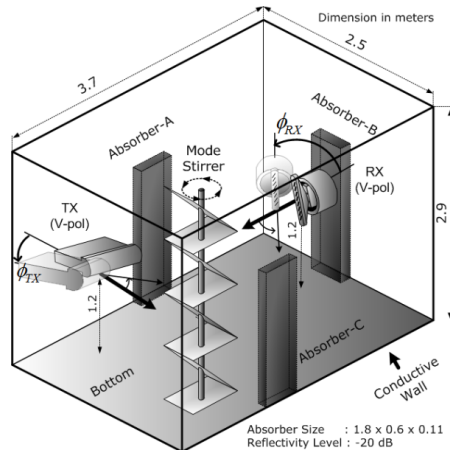


Fig. 1. Experimental campaign in the reverberation chamber.

In the Rayleigh fading, the direct coupling components between TX and RX are negligibly small compared with scattered components. Due to the presence of the absorber, the clustered area in the reverberation chamber is changed; when the absorber is increased, the clustered area becomes small and the transmitted signal decays rapidly. Fig. 2 shows the measured envelope distribution in the Rayleigh fading. The probability density functions of the measured  $S_{IF}$  are consistent with Rayleigh distribution when the number of absorber is decreased.

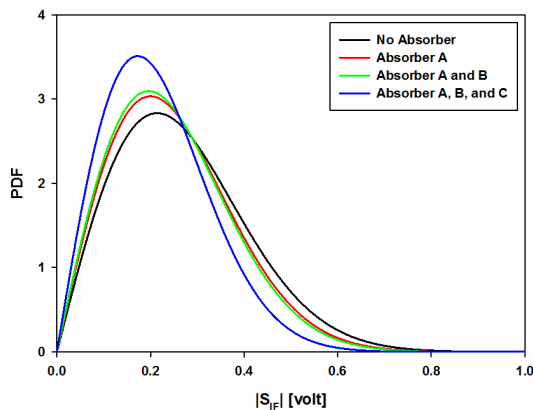


Fig. 2. Envelope distribution in Rayleigh fading at 28.084GHz

In the Rician environment, the strength of one signal path is stronger than the others. RX antenna receives the transmitting signal after one reflection from the conductive wall in company with other scattered signals. The received

power decreases exponentially as the excess delay time is increased. The measured envelope distributions in the some scenarios are well matched with the theoretical Rician distribution and are compared in Fig. 3. In order to analyze the effect of the body tissue in 28GHz propagation, the absorbers are replaced with man at each position.

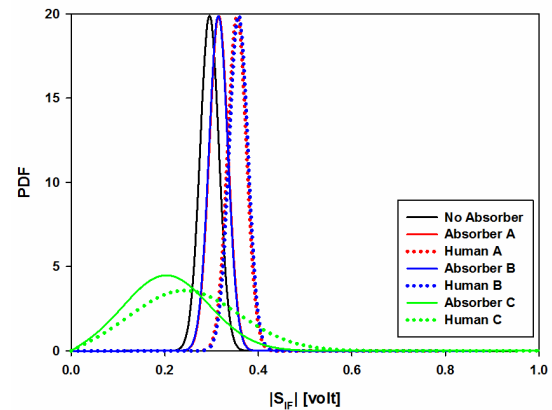


Fig. 3. Envelope distribution in Rician fading at 28.084GHz

#### IV. CONCLUSIONS

We have investigated the variation of the envelope distribution in the Rayleigh and Rician fading at 28GHz band. Based on the unique property of the LFM, the scattering parameter of the system could be obtained by the  $S_{IF}$  of the FMCW radar system. The effect of the body tissue for 28GHz propagation in the LOS propagation was analyzed.

#### ACKNOWLEDGMENT

This work was supported by the National Research Foundation of Korea(NRF) grant funded by the Korea government(MSIP) (No. 2013R1A2A1A01014518.).

#### REFERENCES

- [1] Rappaport, T. S., Murdock, J. N., and Gutierrez, F., "State of the Art in 60 GHz Integrated Circuits & Systems for Wireless Communications," *Proceedings of the IEEE*, vol. 99, no. 8, pp. 1390-1436, 2011.
- [2] Zhouyue Pi, and Khan, F., "An Introduction to Millimeter-Wave Mobile Broadband Systems," *IEEE Communications Magazine*, vol.49, no.6, pp.101-107, 2011.
- [3] S. Salous, S. Feeney, N. Razavi-Ghods, and M. Abdalla, "Sounders for MIMO Channel Measurements," *European Signal Processing Conference*, Florence, Italy, 2006.
- [4] Yun-Taek Im, Ali M., and Seong-Ook Park, "Slow Modulation Behavior of the FMCW Radar for Wireless Channel Sounding Technology," *IEEE Trans. Electromagnetic Compatibility*, 2014.
- [5] S. M. Feeney and S. Salous, "Implementation of a channel sounder for the 60 GHz band," *Proc. URSI XXIX Gen. Assem.*, Chicago, 2008.
- [6] C. L. Holloway, H. A. Shah, R. J. Pirkl, K. A. Remley, D. A. Hill, and J. Ladbury, "Early time behavior in reverberation chambers and its effect on the relationships between coherence bandwidth, chamber decay time, RMS delay spread, and the chamber buildup time," *IEEE Trans. Electromagn. Compat.*, vol. 54, no. 4, pp. 714-725, 2012.